Original Article

JCBFM

Journal of Cerebral Blood Flow & Metabolism
2020, Vol. 40(5) 1077–1089

DOI: 10.1177/0271678X19858888
journals.sagepub.com/home/jcbfm
SAGE

Treatment with dimethyl fumarate reduces the formation and rupture of intracranial aneurysms: Role of Nrf2 activation

Crissey L Pascale[1,*], Alejandra N Martinez[1,*], Christopher Carr[1], David M Sawyer[1], Marcelo Ribeiro-Alves[2], Mimi Chen[1], Devon B O'Donnell[1], Jessie J Guidry[3], Peter S Amenta[1] and Aaron S Dumont[1]

Abstract

Oxidative stress and chronic inflammation in arterial walls have been implicated in intracranial aneurysm (IA) formation and rupture. Dimethyl fumarate (DMF) exhibits immunomodulatory properties, partly via activation of the nuclear factor erythroid 2-related factor 2 (Nrf2) pathway which reduces oxidative stress by inducing the antioxidant response element (ARE). This study evaluated the effects of DMF both in vitro, using tumor necrosis factor (TNF)-α-treated vascular smooth muscle cells (VSMC), and in vivo, using a murine elastase model to induce aneurysm formation. The mice were treated with either DMF at 100 mg/kg/day P.O. or vehicle for two weeks. DMF treatment protected VSMCs from TNF-α-induced inflammation as demonstrated by its downregulation of cytokines and upregulation of Nrf2 and smooth muscle cell markers. At higher doses, DMF also inhibited the pro-proliferative action of TNF-α by increasing apoptosis which protected the cells from aponecrosis. In mice, DMF treatment significantly decreased the incidence of aneurysm formation and rupture, at the same time increasing Nrf2 levels. DMF demonstrated a neuroprotective effect in mice with a resultant inhibition of oxidative stress, inflammation, and fibrosis in the cerebrovasculature. This suggests a potential role for DMF as a rescue therapy for patients at risk for formation and rupture of IAs.

Keywords

Dimethylfumarate, Nrf2, intracranial aneurysm, elastase mouse model, vascular smooth muscle cells

Received 16 April 2019; Revised 3 May 2019; Accepted 27 May 2019

Background

Intracranial aneurysms (IA) are present in approximately 2–5% of the population and when ruptured, subarachnoid hemorrhage (SAH) often results in debilitating neurologic deficit or death.[1,2] Microsurgical and endovascular intervention have advanced significantly, yet both modalities remain associated with significant morbidity and mortality. As a result, the development of non-invasive pharmacological therapy capable of preventing aneurysmal progression and rupture remains a focus of research. Elucidation of the mechanisms underlying IA pathogenesis may provide new targets for intervention. Recent studies have implicated chronic inflammation

[1]Department of Neurosurgery, Tulane Center for Clinical Neurosciences, Tulane University School of Medicine, New Orleans, LA, USA
[2]Laboratory of Clinical Research on STD/AIDS, National Institute of Infectology Evandro Chagas (INI)-Oswaldo Cruz Foundation (FIOCRUZ), Rio de Janeiro, RJ, Brazil
[3]Louisiana State University Health Sciences Center Proteomics Core Facility, New Orleans, LA, USA
[*]These authors contributed equally to this work.

Corresponding author:
Aaron S Dumont, Tulane University, 131 S. Robertson St., Suite 1300, New Orleans, LA 70112, USA.
Email: adumont2@tulane.edu

in arterial walls caused by hemodynamic stress as a factor in IA formation. This inflammation leads to endothelial dysfunction followed by vascular smooth muscle cell (VSMC) phenotypic modulation, extracellular matrix remodeling, and cell death. These cellular processes manifest as vessel wall degeneration, dilation, and eventual rupture.[3] Reactive oxygen species (ROS) are a major mediator of inflammation and have been recognized as intracellular signaling molecules involved in the physiological repair processes after vascular injury.[4–6] The inflammatory reaction associated with IA formation involves extensive ROS production.[3]

Dimethyl fumarate (DMF) is an oral fumaric acid ester that exhibits immunomodulatory properties and is considered a safe therapeutic option for treating patients with psoriasis and relapsing-remitting multiple sclerosis.[7] Previous studies have demonstrated multiple pathways through which DMF acts, including activation of the nuclear factor erythroid 2-related factor 2 (Nrf2). Nrf2 activation reduces oxidative stress by inducing the antioxidant response element (ARE) which promotes the expression of a number of downstream detoxification enzymes such as glutathione, heme oxygenase (HO), and NADPH quinone oxidoreductase 1 (NQO1).[5,8–10] Under normal physiological circumstances, Kelch-like ECH-associated protein 1 (Keap1) functions as a substrate adaptor protein for the Cullin 3 (*Cul3*)/E3 ubiquitin ligase complex to target Nrf2 for proteosome-mediated degradation and is a key negative regulator of Nrf2.[11] DMF can covalently bind to Keap1, allowing Nrf2 to travel to the nucleus and bind to ARE.[6,12]

By activating Nrf2, DMF can minimize brain damage after experimental stroke, subarachnoid and intracerebral hemorrhage, and traumatic brain injury.[13–18] In rats, DMF was shown to be protective against neointimal hyperplasia after vascular injury, preventing VSMC proliferation via Nrf2-regulated modulation of the cell cycle. DMF also protected against tumor necrosis factor-α (TNF-α)-induced apoptosis and endothelial cell dysfunction through Nrf2-NQO1 activity.[5] The beneficial antioxidant and anti-inflammatory effects of DMF have not yet been reported in regards to IA, where the inflammatory response is a key contributor to the changes in the architecture of the arterial wall, including hyperplasia and disarray of VSMCs in the tunica media.[19] Thus, we hypothesize that DMF could prevent inflammatory VSMC phenotypic modulation in vitro and formation and rupture of IAs in vivo in a murine elastase aneurysm model.

Methods

In vitro DMF treatment

C57BL/6 mouse primary brain smooth muscle cells (Cell Biologics, C57-6085) were cultured in DMEM (low glucose) supplemented with 10% (v/v) FBS and antibiotics (100 U/mL penicillin, 100 mg/mL streptomycin) at 37°C in a humidified, 5% CO2 incubator.[20] Cells between the third and sixth passages were used in all experiments. VSMCs were plated in 12-well plates at 1×10^5 cells/well and, once attached, were starved for 2 h in serum-free media containing DMEM/F12, L-ascorbic acid (200 μM), apotransferrin (5 μg/ml) and selenium selenite (6.25 ng/ml). They were subsequently treated with TNF-α (50 ng/mL) and/or DMF (20 μM, 50 μM, 75 μM and 100 μM; Sigma-Aldrich, T5944) in culture medium containing ≤0.001% DMSO for 24 h. The dose of TNF-α was chosen based on prior publications from our group.[20]

Real-time RT-PCR

RNA from VSMCs was extracted using Trizol reagent (ThermoFisher Scientific, 15596026) according to the manufacturer's instructions. Similarly, the circle of Willis tissue from two mice was collected and pooled for RNA extraction. The pooled tissue was homogenized using a Scilogex D160, and RNA was extracted with Trizol reagent. DNase post-treatment was performed on all the samples using a DNA-free™ kit (ThermoFisher Scientific, AM1906) to remove genomic DNA contamination. cDNA was prepared with 0.5 μg total RNA per reaction using a Transcriptor First Strand cDNA kit (Roche Diagnostics, 04379012001), and mRNA expression was quantified with SYBR Green (Roche Diagnostics, 06402712001) on a Light Cycler 96 real-time system (Roche Diagnostics) and normalized to the average expression of beta-actin and beta2-microglobulin housekeeping genes. Experiments were performed in triplicate with $n = 9$ samples per group.

Immunodetection of chemokines and cytokines

Cell culture supernatant from VSMCs was analyzed using a commercially available multiplex bead-based immunoassay (Bio-Plex Pro™ Mouse Cytokine 23-plex Group 1; Biorad, m60009rdpd). Briefly, coupled beads were incubated for 2 h at room temperature (RT) with the VSMC supernatants or recombinant standards of each chemokine. After washing, a biotinylated detection antibody was added to the reaction. A streptavidin-phycoerythrin (PE) reporter complex

was then added to reveal the biotinylated detection antibodies. PE fluorescence was analyzed on a Bioplex-200 analyzer (Bio-Rad), and the levels of bound analytes were quantified using standard curves obtained with the recombinant chemokines.

Annexin V-FITC/PI staining for apoptosis detection

The rate of VSMC cell apoptosis after DMF treatment was evaluated using Annexin V-FITC Apoptosis Detection Kit (Sigma, APOAF). Following treatment with different concentrations of DMF, the cells were harvested, washed with PBS and resuspended in 100 µL binding buffer. Then the cells were incubated in the dark with Annexin V and PI for 10 min and analyzed using flow cytometry. Three parallel wells were used per sample.

In vivo DMF treatment

Eight-week-old, male, C57BL/6 mice were obtained from Jackson Laboratories. Mice were randomly assigned to be treated with either DMF (Sigma Aldrich, 242,926) at 100 mg/kg/day orally or vehicle,[21,22] 1% carboxymethylcellulose (CMC) (Sigma Aldrich, C9481), from the time of aneurysm induction until sacrifice, two weeks later ($n = 60$). CMC was used as a thickening agent to form a colloidal mixture with DMF which was administered by oral gavage at a volume of 0.2 mL. There was an additional cohort of sham-operated controls ($n = 15$). At the conclusion of the study, the mice were anesthetized and transcardially perfused with a phosphate-buffered saline (PBS) solution containing 4% gelatin and 2 mg/mL bromophenol blue in order to visualize the cerebral vessels. Under a microscope, the number and nature of any aneurysms were noted and photos were taken of the ventral side of the brains. Researchers were blinded to treatment groups. The circles of Willis were then harvested for downstream molecular analyses.

Elastase aneurysm model

Animal surgery procedures were approved by the Tulane University Institutional Animal Care and Use Committee. All animal research was performed in accordance with the National Institute of Health's guide for the care and use of laboratory animals and in compliance with Animal Research: Reporting in Vivo Experiments guidelines. For all survival surgeries, anesthesia was established using ketamine and xylazine at 100 and 10 mg/kg, respectively. To induce aneurysm formation in mice, we used a well-established model that involves pharmacologically inducing hypertension and then stereotactically injecting elastase into the basal cistern.[23] To induce hypertension, the mice underwent a unilateral nephrectomy followed by implantation of a deoxycorticosterone acetate (DOCA) pellet (Innovative Research of America; M-121 50 mg, 21 day release) in the subcutaneous tissue of the interscapular region one week later. Also, at this time, the mice were given 1% NaCl in their drinking water and elastase (Sigma Aldrich; E7885) was injected into the basal cistern. To perform this, the tip of a 26 g needle was positioned using the following coordinates on a stereotaxic frame: 1.3 mm lateral to the midline, 2.6 mm posterior from bregma and 6 mm ventral to the skull, and elastase (17.5 mU in 2.5 µL sterile saline) was injected at a rate of 0.2 µL/min. Mice were excluded from the study if they did not recover within 72 h after the stereotactic injection.

Radiotelemetry blood pressure recording

A subset ($n = 5$) of all animal groups underwent an additional surgery two weeks prior to aneurysm induction where a radiotelemetry (Data Sciences International [DSI], TA11PA-C10) probe was implanted. This enabled remote measurements of blood pressure in conscious mice. In brief, the transmitter lead was inserted into the left carotid artery, advanced to the level of the aortic arch, and secured with suture. The implant itself was positioned under the skin of the right flank.[24] The blood pressure of the mice was allowed to return to baseline before aneurysm induction, and recordings were measured once a week thereafter until sacrifice. DSI Ponemah v6.4 software was used to collect the data.

Immunocytochemistry and confocal microscopy

A subset ($n = 2$) of mice had the entire brain harvested for immunohistochemistry. They were placed in 4% paraformaldehyde overnight (o/n), followed by 15% sucrose for 24 h, and, finally, 30% sucrose for 24 h. They were then placed in OCT media and frozen using liquid nitrogen. Coronal sections were obtained at a thickness of 16 µm. Representative brain sections were blocked for 1 h using blocking buffer (PBS containing 1% BSA, 0.1% cold fish skin gelatin, 0.5% Triton X-100 and 0.05% sodium azide) and, subsequently, incubated with the following primary antibodies: anti-actin α-smooth muscle (Sigma Aldrich A2547; 1:200 dilution) and anti-Nrf2 (Abcam ab31163; 1:50 dilution) for 2 h at RT. Alexa Fluor 488 and 594 secondary antibodies (1:600; Life

Technologies) were applied for 1 h, followed by nuclear labeling with DAPI (1:300; Life Technologies) for 5 min. ProLong Gold mounting media (Life Technologies) was used to prevent photobleaching during imaging. Stained slides were imaged using the Nikon eclipse Ti2 confocal microscope.

Protein extraction from circle of Willis arteries

Proteins were extracted from surgically isolated arteries by adding 100 µL of 0.2% (w/v) Rapigest SF (Waters, USA) in 50 mmol/L ammonium bicarbonate. The mixture was then exposed to three, 20 s pulses of sonication to further facilitate protein extraction. The above steps were all performed on ice. Each preparation was then incubated at 95°C for 10 min, followed by a 20 min centrifugation at 10,000*g*.[25] Cerebral arteries from three mice were combined to constitute one biological replicate. The total protein concentration from 12 biological replicates was determined using Bicinchoninic Acid (BCA) assay in microplate format using an 8-point standard curve of bovine serum albumin (BSA) in duplicate; 100 µg of each sample was aliquoted and reduced with 10 mM Tris (2-carboxyethyl) phosphine (TCEP) for 1 at 55°C. Cysteines were alkylated with 20 mM Iodoacetamide (IAA) at RT for 30 min in the dark. The protein aliquots were desalted using methanol/chloroform extraction[26] before drying to completion in a speed vacuum concentrator. The dried pellets were dissolved o/n at 37°C in 2 µg of mass spectrometry grade trypsin protease in 100 mM TEAB.

Mass spectrometry (LC-MS)

Samples were labeled and fractioned using tandem mass tags (TMTs) as per the manufacturer's specifications (Thermo Scientific, Waltham, MA). Following labeling, an equal amount of each lysate was pooled together, SepPak purified to eliminate salts, and then subjected to fractionation by basic pH reverse phase HPLC (bpH-HPLC). For bpH-HPLC, the pooled sample was resuspended in 260 µl of 10 mM ammonium hydroxide, pH10, and subjected to basic pH reverse phase chromatography (Dionex U3000, Thermo Fisher) using an ACQUITY UPLC Peptide BEH C18 Column, 300 A, 1.7 µm, 2.1 mm × 50 mm (Waters, Ireland). A total of 48 fractions were collected in a 96-well microplate and recombined in a checkerboard fashion to create the 12 "super fractions."[27] The super fractions were run on a Dionex U3000 nano flow system coupled to a Thermo Fusion mass spectrometer and subjected to a 90 min chromatographic method employing a stepwise gradient from 2 to 25% of acetonitrile in 0.1% formic acid (ACN/FA) over the course of 65 min, a gradient to 50% ACN/FA for an additional 10 min, a step to 90% ACN/FA for 5 min and a 10 min re-equilibration into 2% ACN/FA. Chromatography was carried out using a PicoChip source (New Objective,) in a trap-and-load format where the trap column was the C18 PepMap 100, 5 µm, 100A and the separation column was PicoChip REPROSIL-Pur C18-AQ, 3 µm, 120A, 105 mm. The entire run was 0.3 µl/min flow rate.

Peptide and TMT data acquisition utilized a MS3 approach for data collection and survey scans (MS1) were performed in the Orbitrap utilizing a resolution of 120,000 between 375 and 1600 m/z. Data dependent MS2 scans were performed in the linear ion trap using a collision-induced dissociation (CID) of 25%. Reported ions were fragmented using high energy collision dissociation (HCD) of 65% and detected in the Orbitrap using a resolution of 50,000. This was repeated for a total of three technical replicates. TMT data analysis was performed using Proteome Discoverer 2.2. The 3 runs of 12 "super fractions" were merged and searched using SEQUEST. The Protein FASTA database was Mus musculus (NCBIAV Tax ID = 10090) version 2017-05-05. Static modifications included TMT reagents on Lysine and N-terminus (+229.163), carbamidomethyl on cysteines (= 57.021), and dynamic modification of oxidation of methionine (= 15.9949). Parent ion tolerance was 10 ppm, fragment mass tolerance was 0.6 Da, and the maximum number of missed cleavages was set to 2. Only high scoring peptides were considered utilizing a false discovery rate (FDR) of 1%.

Log_{10} mean intensity transformed values generated by mass spectrometry (LC-MS) assays were modeled by fixed-effects ('Aneurysm' and 'DMF') two-way ANOVA with a first-order interaction term and results were presented by the expected marginal mean values ± its 95% confidence intervals (CI 95%). Hypothesis for contrasts generated from the expected mean values of the experimental groups were tested by Tukey's honest significant pairwise tests. Differentially expressed proteins were profiled by a Bayesian infinite mixture model cluster.[28] To identify mechanisms potentially involved in the aneurysm formation and/or rupture either in treatment with DMF or not, GO enrichment analysis were performed. The gene set comprised genes encoding differential expressed proteins revealed in the previous analysis, and the universe comprised all genes encoding proteins detected by LC-MS assays in all samples. Mapping among genes and encoding proteins was based on Bioconductor Mus musculus package 'org.Mm.eg.db'.[29] Overrepresented biological processes (BP), molecular functions (MF), and cellular components (CC) were identified based on a hypergeometric test with p-values ≤ 0.001. Identical analyses were performed also for gene sets

comprising genes within profiled clusters. LC-MS assay analysis was performed in R version 3.4.4. Canonical pathway analysis was performed using ingenuity pathway analysis (IPA) tool from the Ingenuity Systems.[30] All hypothesis tests were two-sided and p-values ≤ 0.1, 0.05, and 0.01 were considered suggestive, significant, and highly significant, respectively.

Statistical analysis

For the continuous values generated by real-time RT-PCR, immunodetection, and Annexin V-FITC/PI staining assays, hypotheses were tested by one-way ANOVA followed by multiple t-tests. For the in vitro experiments, each experimental group was compared to the TNF-α-stimulated control group and for the in vivo experiments, each experimental group was compared to the sham group. The p-values were adjusted using Bonferroni correction.

For the continuous variables generated by radiotelemetry blood pressure recording, the hypothesis was tested independently at each week (0 to 3) by one-way ANOVA, followed by Tukey's honest significance tests comparing each experimental group with the sham-operated control group. Results are presented as mean ± standard deviation. The frequency of mice suffering aneurysm formation and/or rupture between the DMF treated group and the saline vehicle-treated control were compared by Fisher's exact hypothesis tests of association. Results were presented as mean frequency and its interquartile interval. All of the above analyses were performed with SAS version 9.4 and p values of ≤ 0.05 were considered significant. Primary analysis of treatment efficacy was compared by Fisher's exact hypothesis tests of association. Results were presented by its mean frequency and its interquartile interval. We calculated 95% confidence intervals for relative risk (RR), relative risk reduction (RRR), absolute risk reduction (ARR), and number needed to treat (NNT).

Results

DMF inhibits the pro-inflammatory cytokine production and the pro-inflammatory, pro-proliferative phenotype induced by TNF-α in primary murine VSMCs

To explore the effects of DMF on VSMCs, we cultured primary cells from cerebral blood vessels, stimulated them with a previously determined concentration of TNF-α (50 ng/ml) and treated them with different concentrations of DMF for 24 h. Gene expression analysis confirmed that TNF-α prompted cell dysfunction by up-regulating the inflammatory markers, chemokine (C-C motif) ligand (CCL)-2, matrix metalloproteinase (MMP)-2 and vascular cell adhesion molecule (VCAM) (Figure 1(a) to (c)), and down-regulating the SMC markers, SM-α-actin and SM-MHC (Figure 1(d) to (f)). This effect was significantly improved by treatment with DMF in a dose-dependent manner. Additionally, we found that DMF treatment increased Nrf2 expression in both TNF-α-stimulated VSMCs and unstimulated cells (Figure 1(d) and Suppl. Figure 4).

To confirm the anti-inflammatory effect of DMF, we measured the release of cytokines and chemokines in the culture supernatants collected at 24 h. TNF-α stimulus up-regulated only CCL2, CCL5 and chemokine (C-X-C motif) ligand (CXCL)-1, suggesting that it plays a role in the synthesis of chemokines involved in subsequent cell recruitment. DMF treatment was able to significantly down-regulate the release of those chemokines (Figure 2(a) to (c)). Taken together, these data suggest that resident tissue cells, such as VSMCs, influence the evolution of the inflammatory response established in the cerebral blood vessels of IAs. Moreover, DMF was able to suppress the phenotypic modulation of VSMCs involved in the pathogenesis of IAs, at least in part, by stimulating Nrf2 activity.

Previously, DMF was reported to inhibit VSMC proliferation in vitro through G0/G1 cell cycle arrest.[5] We examined cell death rates, in order to investigate whether DMF-induced inhibition on cell growth was exclusively due to cell cycle arrest or not. We found that the proportion of apoptotic VSMCs increased, while the proportion of aponecrotic cells decreased after DMF treatment at the concentrations of 75 and 100 μM, not at the lower doses of DMF (Figure 3(a) and (b); $p \leq 0.05$). The number of VSMCs also decreased with increasing DMF concentration, as assessed by total cell count using flow cytometry (Figure 3(c); $p \leq 0.05$). This finding corroborates the known effect of DMF on cell growth.

DMF treatment induces immune modulation in IAs through activation of the Nrf2 pathway

Preclinical studies and our in vitro model demonstrated that DMF activates the nuclear Nrf2 pathway, and thus regulates the antioxidant response.[5,31,32] In our in vivo model, the induction of IA significantly upregulated Nrf2 expression and this increase was significantly higher in the DMF-treated group (Figure 4(a); $p \leq 0.001$). Under quiescent conditions, Nrf2 is anchored in the cytoplasm through binding to Keap1, which facilitates its ubiquitination and subsequent proteolysis. In view of this, we demonstrated that Keap1 transcription levels are reduced in the DMF-treated animals compared to the vehicle-treated group (Figure 4(b); $p \leq 0.05$).

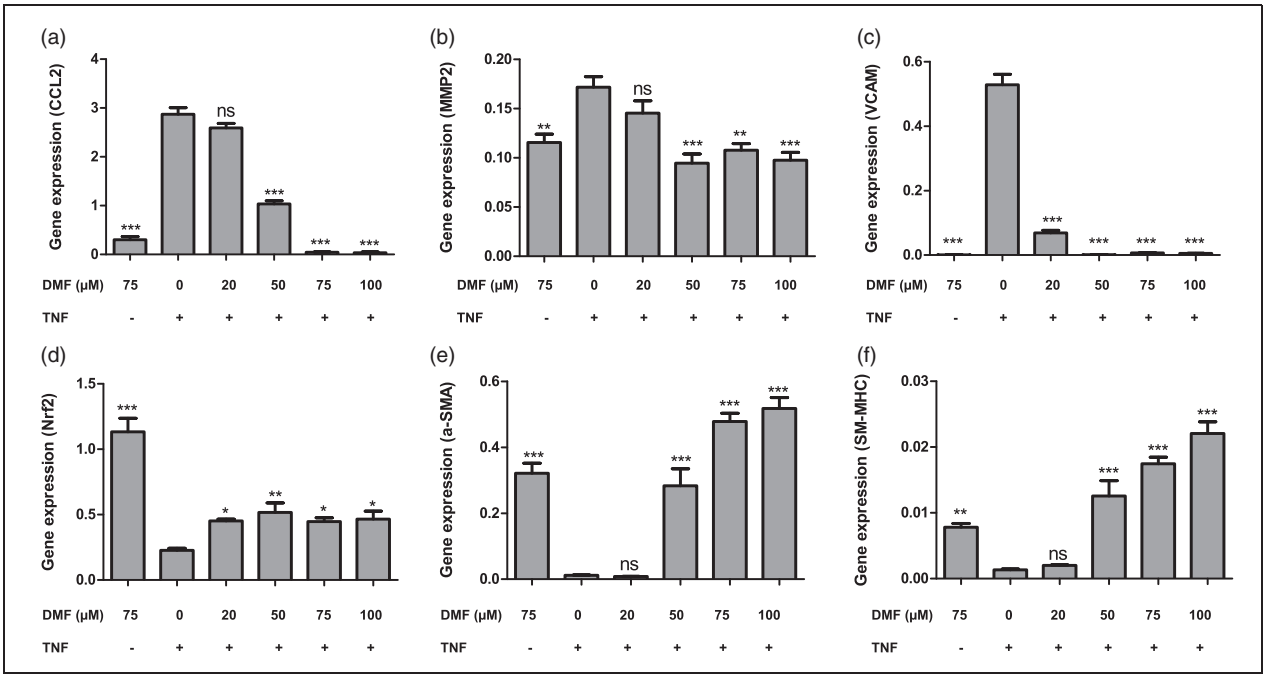

Figure 1. DMF alters cytokine gene expression profiles, as well as the pro-proliferative antioxidant response induced by TNF-α in VSMCs. Cells were treated for 24 h with 20, 50, 75 or 100 μM DMF and mRNA quantitated by RT-PCR. (a) MCP1, (b) MMP2, (c) VCAM, (d) Nrf2, (e) a-SMA and (f) SM-MHC. The data were assessed from three independent experiments. Asterisks (*$p < 0.05$; **$p < 0.01$, ***$p < 0.001$), indicate significant differences compared to cells stimulated solely by TNF-α (ANOVA followed by the Bonferroni test).

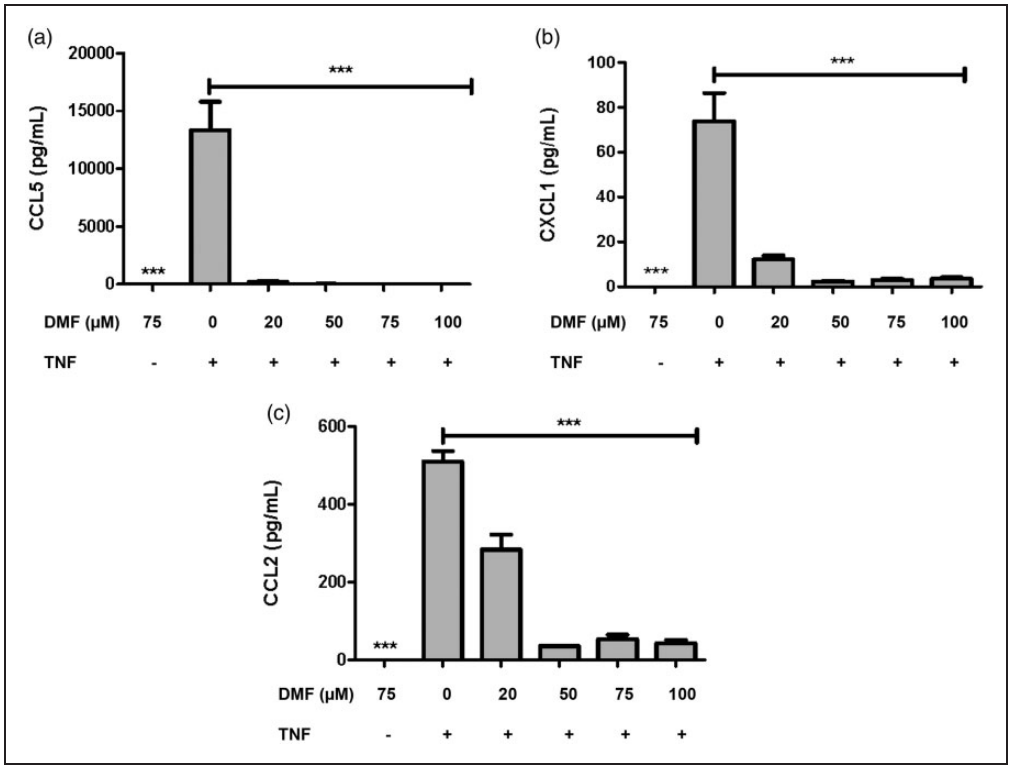

Figure 2. DMF modulates the inflammatory release of cytokines and chemokines induced by TNF-α in culture supernatants from VSMCs. Cells were treated for 24 h with 20, 50, 75 or 100 μM DMF and protein release was measured by the BioPlex assay. (a) CCL5, (b) CXCL1 and (c) CCL2. The data were assessed from three independent experiments. ***$p < 0.001$ indicates significant differences compared to cells stimulated solely by TNF-α (ANOVA followed by the Bonferroni test).

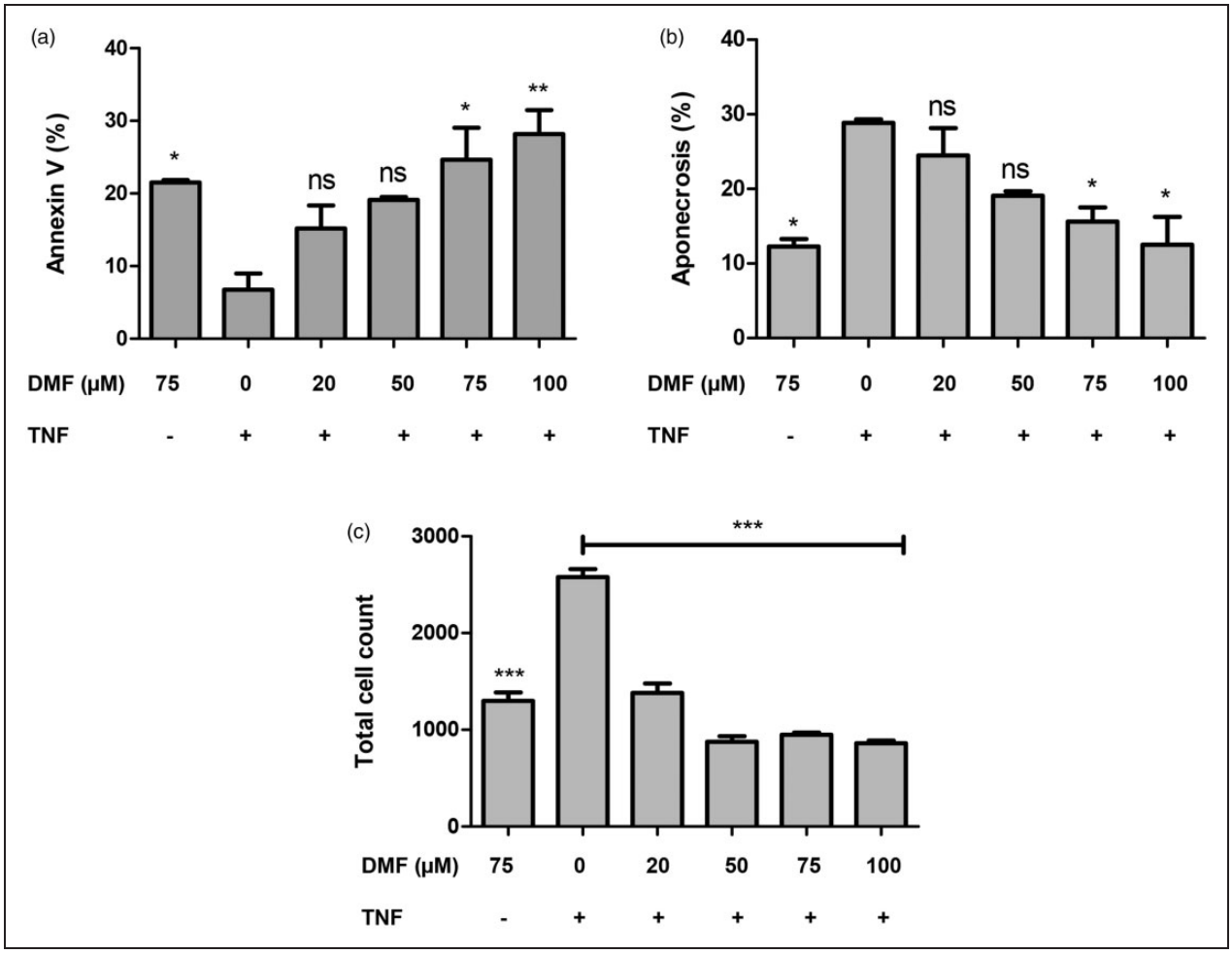

Figure 3. DMF increases apoptosis while protecting VSMCs from aponecrosis. Cells were treated for 24 h with 20, 50, 75 or 100 μM DMF and cell death assessed by Annexin V/PI staining followed flow cytometry detection. (a) Percentage of apoptotic cells measured by Anexin V positive, (b) Percentage of aponecrotic cells measured by PI and AnnexinV positive, (c) Absolute cell count. Asterisks (*$p < 0.05$; **$p < 0.01$, ***$p < 0.001$), indicate significant differences compared to cells stimulated solely by TNF (ANOVA followed by the Bonferroni test).

We also investigated the effect of DMF at the protein level by using quantitative discovery-based proteomics. A total of 3457 proteins were identified in cerebral arteries from treated and untreated mice using a 1% FDR. Hierarchical cluster analysis identified groups of proteins that showed similar patterns in regard to the effect of DMF (Figure 5) and we focused on cluster 5 due to the significant differences between the treatment groups associated with aneurysm formation/rupture. IPA was used to identify enriched biological processes and canonical pathways associated with cluster 5. Among the most significant canonical pathways we found were actin cytoskeleton signaling, rho signaling and the Nrf2-mediated oxidative stress response (Table 1). The interplay between these pathways involves the regulation of actin cytoskeleton by Rho proteolysis in response to oxidative stress.[33] Furthermore, from the list of interacting proteins associated with Nrf2 pathway, we found significantly decreased levels of Cul3 in the DMF-treated group compared to non-treated group (Suppl. Table 1, Figure 1 and Suppl. Figure 4). This correlates with a decreased association of Keap1 with Cul3 and, thus, a decreased inhibition of Keap1-dependent ubiquitination of Nrf2 in the DMF-treated group leading to the accumulation of Nrf2. Hence, our proteomics results suggest that DMF acts by modulating Nrf2 levels, leading to a protective response to cell stress through reorganization of the actin cytoskeleton. Histologic features of vessel walls harboring IAs include chronic inflammatory cell infiltration of the adventitia and media layers, elastin fragmentation, degeneration, and attenuation of the media. Collagen synthesis increases during the early stages of aneurysm formation suggesting a repair process. In addition, fibrosis primarily results from type I collagen deposition. Accordingly, IA formation significantly

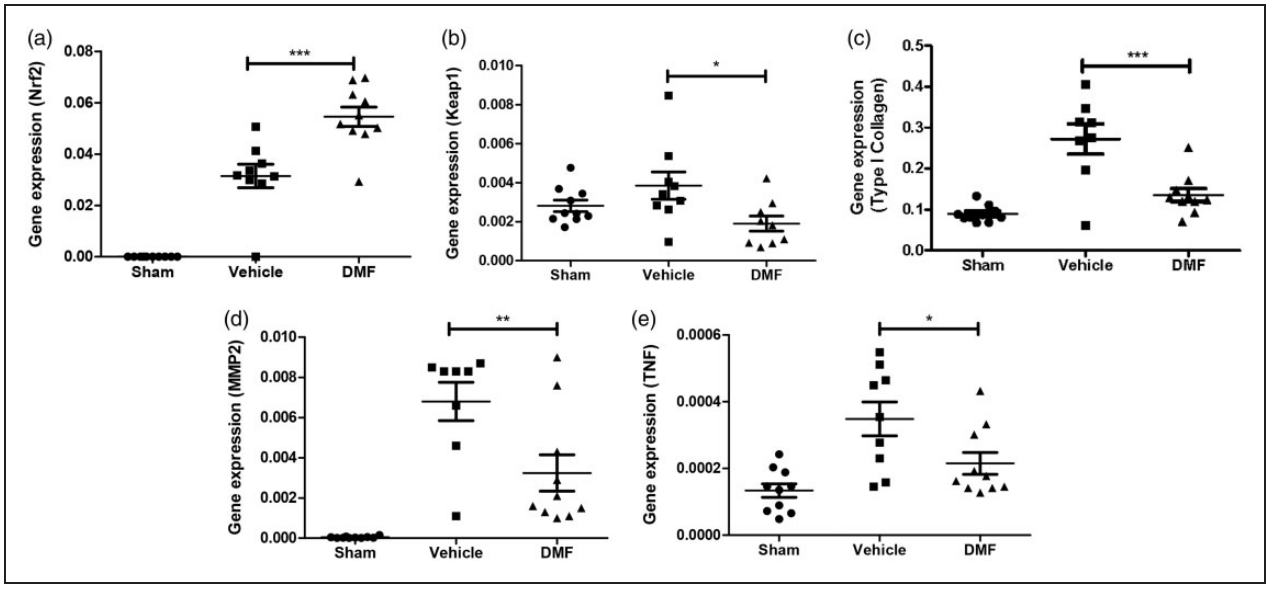

Figure 4. DMF modulates the expression of genes known to be essential for inflammation, oxidative damage, and fibrosis in the experimental model of IA. (a) Nrf2, (b) Keap1, (c) Type I Collagen, (d) MMP2 and (e) TNF-α. Quantitative RT-PCR from vehicle-treated and DMF-treated groups (with or without aneurysm) was compared to cerebral artery tissue from sham-operated group ($n = 9$). Comparisons between the three groups were made using ANOVA followed by the Bonferroni test (*$p < 0.05$; **$p < 0.01$, ***$p < 0.001$).

Table 1. Top canonical pathways from cluster 5.

Top canonical pathways	*p* value	Overlap
Actin cytoskeleton signaling	9.82E-04	1.8% 4/224
RhoA signaling	1.68E-03	2.5% 3/119
RhoGDI signaling	4.69E-03	1.8% 3/171
D-glucuronate degradation I	5.94E-03	33.3% 1/3
Nrf2-mediated oxidative stress response	6.19E-03	1.6% 3/189

upregulated type I collagen gene expression in our model, and this increase was significantly lower in the DMF-treated group (Figure 4(c); $p \leq 0.001$). Similarly, IA induction increased the expression of the inflammatory genes MMP2 and TNF-α and this increase was significantly lower in the DMF-treated group (Figure 4(d) and (e); $p \leq 0.01$ and $p \leq 0.05$, respectively). Taken together, these in vivo results suggest that DMF modulates the expression of genes known to be essential for inflammation, oxidative damage, and fibrosis in the experimental models of IA, reducing the contributions of pathogenic pathways.

DMF treatment significantly reduced the number of aneurysms formed and ruptured in an elastase mouse model

To determine if the beneficial anti-inflammatory effects of DMF seen in vitro could also be demonstrated in an in vivo murine model of cerebral aneurysms, we treated mice with DMF, or a vehicle control, following aneurysm induction. Results showed a significant reduction in the number of aneurysms formed in the DMF-treated group compared to the control group (Figure 6(a)). Seventy percent of the control mice formed aneurysms (42/60), whereas only 51% of the DMF-treated mice formed aneurysms (31/61) ($p \leq 0.05$). An even stronger difference was seen in the number of mice that experienced aneurysmal rupture: 64% (38/60) of the control mice experienced SAH vs. 43% (26/61) of the DMF-treated mice ($p \leq 0.05$; RR = 0.67, 95%CI = 0.47–0.95; NNT = 5). There was no significant difference in mean arterial blood pressure (MAP) between the two groups (Figure 6(b)). Representative images of mouse brains (Figure 6(c)) depict normal intracranial vasculature, IA formation without rupture, and SAH due to IA rupture.

Discussion

In normal arteries, the endothelium maintains the integrity of the vessel lumen, while the VSMCs play a crucial role in the contractility of the arterial wall. VSMCs, working in conjunction with fibrous layers of collagen and elastin, give arteries the plasticity needed to withstand hemodynamic stress.[34] This structural integrity is lost in IAs, as the infiltration of inflammatory cells induces a VSMC phenotypic switch from a contractile, to a more proliferative and pro-inflammatory state, where the extracellular matrix becomes

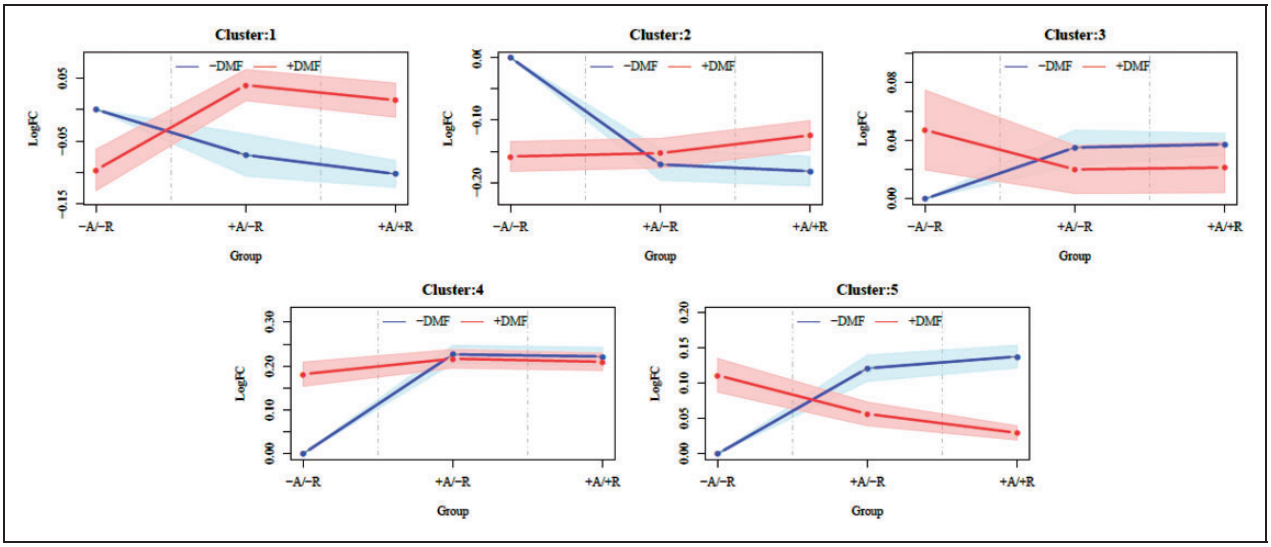

Figure 5. Cluster profiles of differentially expressed proteins from Circle of Willis arteries in elastase aneurysm model mice either treated with DMF (red) or vehicle (blue). Five clusters were defined by a Bayesian infinite mixture model clustering algorithm [ref.]. Y-axis are log (base 10) fold-changes among mean intensity values (solid lines) ± CI 95% (shaded polygons) of clusters of differentially expressed proteins generated by mass spectrometry (LC-MS) assays of mice either with (+) or without (−) aneurysm formation (A) and rupture (R) either treated with DMF (+DMF) or vehicle (−DMF) and mean intensity values of controls (−A/−R/−DMF).

remodeled.[35] DMF (Tecfidera) is an FDA-approved oral fumarate ester that has several pharmacological benefits including immunomodulation and prevention of fibrosis, which are dependent on Nrf2 antioxidant pathways.[36] Here we demonstrated that DMF treatment reduced the pro-inflammatory response and decreased the incidence of formation and rupture of IAs in vivo, and protected VSMCs from TNF-α induced phenotypic modulation in vitro.

Significant progress has been made in understanding VSMC biology and TNF-α has been shown to promote the pro-inflammatory/matrix-remodeling phenotype associated with IA formation.[20] Upregulation of TNF-α in VSMCs leads to increased expression of pro-inflammatory genes and matrix metalloproteinases (MMPs), both of which are identified in human cerebral aneurysms.[20,34,37–39] Here we confirmed that TNF-α induces VSMC dysfunction as evidenced by up-regulating inflammatory markers and down-regulating the expression of SMC markers (Figure 1). DMF treatment successfully suppressed this phenotypic modulation in vitro. We also found DMF treatment to be associated with increased gene expression levels of Nrf2 both in vitro and in vivo (Figures 1, 2 and 6). Nrf2/Keap1-mediated protection against oxidative stress has been previously observed in VSMCs[6,40] and has been shown to regulate VSMC apoptosis during neointimal formation, thereby inhibiting hyperplasia after vascular injury.[6] In this study, higher doses of DMF inhibited the pro-proliferative action of TNF-α on VSMCs via increased apoptosis while protecting the cells from aponecrosis (Figure 3(a) and (b)). We suggest that DMF upregulates the Nrf2/Keap1 system, which reduces IA myointimal hyperplasia by inducing VSMC apoptosis and protecting these cells from inflammatory necrotic cell death.

Inflammation, angiogenesis, and oxidative stress are implicated in the pathogenesis of various vascular diseases. Recent research suggests DMF may be a suitable alternative or complimentary therapy to current interventions. Analysis of the effect of DMF on activated human endothelial cells showed it to be capable of suppressing the TNF-α-induced expression of important cytokines/chemokines.[41] Gene expression profile in the media of aneurysmal walls in a rat model of cerebral aneurysm showed that important mediators, including CCL2, CCL5, and CXCL1 were upregulated in the media.[42,43] CCL2, CCL5, and CXCL-1 play important roles in monocyte accumulation, leukocyte trafficking, and neutrophil recruitment, respectively, and their inhibition is associated with reduced atherogenesis and aneurysm formation in mice.[44,45] We showed that supernatant from VSMC cultures treated with DMF has markedly less secretion of CCL2, CCL5, and CXCL-1 (Figure 2) suggesting that DMF modulates the inflammatory cell influx in vascular lesions associated with IAs.

The pharmacological benefit of DMF was evaluated in an elastase animal model and we found significantly reduced numbers of IAs that formed and ruptured in the treated animals. In addition, untreated mice experienced morbidity and mortality at a quicker rate than

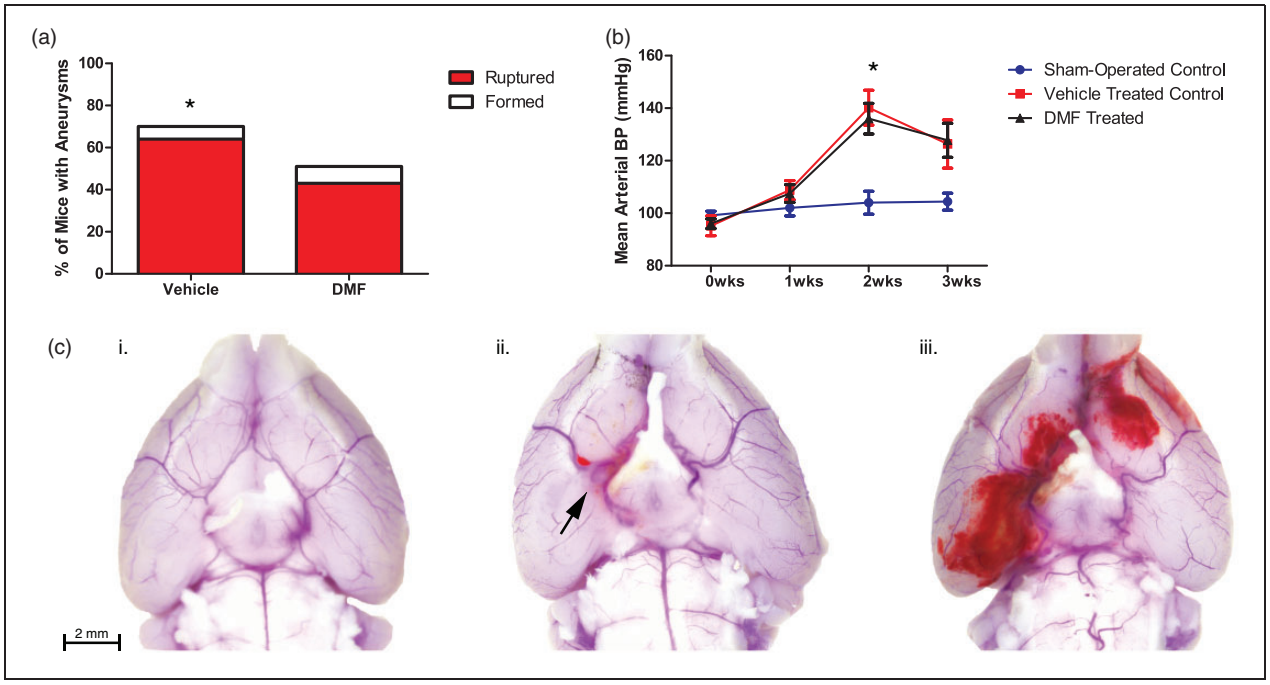

Figure 6. DMF prevents the formation and rupture of IAs in a mouse model without affecting blood pressure. (a) The percentage of aneurysms that formed and/or ruptured in mice treated with either DMF or a vehicle control. Fisher Exact Test was performed (*$p < 0.05$). (b) Mean arterial blood pressure was measured in DMF- and vehicle-treated mice and compared to sham-operated controls. ANOVA followed by Tukey post hoc analysis was performed (*$p < 0.05$). (c) Representative mouse brains demonstrating (i) No aneurysm formation, (ii) Aneurysm formation with no rupture, and (iii) Aneurysmal rupture with SAH.

those treated with DMF (Suppl. Figure 2). This treatment did not have an effect on blood pressure (Figure 6(b)). Gene expression from the circle of Willis showed that DMF treatment significantly upregulated Nrf2 expression while downregulating Keap1 (Figure 4(a) and (b)). The Keap1-Nrf2-ARE pathway has been shown to suppress oxidative stress and inflammatory responses in the brain in different animal models, including SAH models.[16,46–48] Furthermore, animals treated with DMF presented lower levels of MMP2, TNF-α, and type I collagen. In line with the gene transcription results, proteomics enrichment analysis identified the Nrf2-mediated oxidative stress response to be associated with intracranial aneurysm pathogenesis (Table 1). In particular, we noted that Cul3 levels were significantly lower in the DMF-treated group (Suppl. Table 1 and Figure 2) suggesting lower levels of Nrf2, since the ability of Keap1 to assemble into a functional Cul3 ubiquitin ligase complex is a critical determinant that controls steady-state levels of Nrf2.[11] DMF also downregulated the expression of proteins belonging to the Rho family (Table 1) which play central roles in regulating the organization of the actin cytoskeleton.[49,50] Preclinical studies have indicated the benefit of clinical Rho pathway inhibition in the maintenance of vascular tone[51] and suppression of NAD(P)H-induced oxidative stress[52] and our analysis suggests a crosstalk mechanism between Rho kinase and redox signaling that is regulated by DMF. Taken together, our in vivo results indicate that DMF acts by regulating different cellular pathways ultimately leading to immunomodulation and prevention of deposition of type I collagen in the arterial wall that can cause fibrosis in IAs.

In a number of studies, the beneficial effects of DMF were absent in Nrf2-deficient mice, demonstrating a critical role of the Nrf2 pathway in its neuroprotective effects.[12,14,53,54] Nevertheless, DMF has pleiotropic modes of action that have not yet been fully elucidated. DMF has been shown to block pro-inflammatory cytokine production and modulate T and B cells, as well as antigen-presenting cells, and its immunomodulatory effects have been observed in Nrf2 knockout mice.[22,55,56] Moreover, it has been demonstrated that DMF is an agonist of the hydroxycarboxylic acid receptor 2 (HCAR2).[32,57] This receptor is a member of the nicotinic acid receptor family of the G protein-coupled receptors (GPCRs) and its activation inhibits lipolytic and atherogenic activity, induces vasodilation, and decreases the expression of adhesion molecules.[57,58] Also, a very recent discovery has shown that DMF downregulates aerobic glycolysis in activated myeloid and lymphoid cells, which mediates its anti-inflammatory effects. As a metabolic intermediate of the Krebs

cycle, DMF is able to covalently modify cysteine residues from different targets preventing immune activation and shifting the balance between inflammatory and regulatory cell types.[59] Further work is needed to investigate the potential contribution of these alternate pathways of action to the protective effect of DMF observed in this study.

This study was powered to evaluate various dosages of DMF in vitro while only evaluating the impact of a single dose in vivo. Hence, future work will aim to elucidate the optimal therapeutic dose and delineate its effect on aneurysm-related morbidity and mortality. Our elastase mouse model also presents limitations associated with the small animal size and required systemic hypertension that leads to faster IA formation as compared to humans. However, this model is well validated and shares common molecular mechanisms with human IAs allowing investigation of pathogenic mechanisms and therapeutic screening. Taken together, our results have demonstrated therapeutic efficacy of DMF in a murine IA model that may be mediated by the activation of the Keap1-Nrf2-ARE system with a resultant inhibition of oxidative stress, inflammation, and fibrosis in the cerebral vasculature. This suggests a potential role for DMF as a pharmacologic therapy for patients at risk for formation and rupture of IAs.

Funding

The author(s) disclosed receipt of the following financial support for the research, authorship, and/or publication of this article: This study received funding from the Dean's Office and Department of Neurosurgery, Tulane University School of Medicine. The Proteomics Project described was supported by P20 RR018766, P20 GM103514, P30 GM103514, and a special appropriation from the LSU School of Medicine Office of the Dean.

Acknowledgments

The authors would like to thank Alan Tucker and Dina Gaupp of the Tulane Center for Stem Cell Research and Regenerative Medicine for their assistance in performing the flow cytometry and histology for this study.

Declaration of conflicting interests

The author(s) declared no potential conflicts of interest with respect to the research, authorship, and/or publication of this article.

Authors' contributions

CLP and ANM wrote and contributed equally to the manuscript. CLP and ANM designed and performed the experiments and collected and analyzed the data. DMS, MC and DBO performed some experiments and collected the data. JJG performed the proteomics experiments. MRA and CC performed the statistical analysis of the data. PSA participated in the design of the study and helped write the manuscript. ASD is the Principal Investigator and conceptualized the experiments. All authors reviewed and approved the final manuscript.

Ethics approval

This study did not utilize any human participants, human data, or human tissue. Animal surgery procedures were approved by the Tulane University Institutional Animal Care and Use Committee.

Availability of data

Upon request, the raw data from the binary files generated by the mass spectrometer that are then processed by the researcher to yield results such as peak, peptide and protein lists will be made freely available from the laboratory of the senior (corresponding) author.

Supplemental material

Supplemental material for this paper can be found at the journal website: http://journals.sagepub.com/home/jcb

ORCID iD


Jessie J Guidry https://orcid.org/0000-0002-5601-0430

References

1. Molyneux AJ, et al. Risk of recurrent subarachnoid haemorrhage, death, or dependence and standardised mortality ratios after clipping or coiling of an intracranial aneurysm in the International Subarachnoid Aneurysm Trial (ISAT): long-term follow-up. *Lancet Neurol* 2009; 8: 427–433.
2. Wiebers DO, et al. Unruptured intracranial aneurysms: natural history, clinical outcome, and risks of surgical and endovascular treatment. *Lancet* 2003; 362: 103–110.
3. Starke RM, et al. The role of oxidative stress in cerebral aneurysm formation and rupture. *Curr Neurovasc Res* 2013; 10: 247–255.
4. Lyle AN and Griendling KK. Modulation of vascular smooth muscle signaling by reactive oxygen species. *Physiology* 2006; 21: 269–280.
5. Oh CJ, et al. Dimethylfumarate attenuates restenosis after acute vascular injury by cell-specific and Nrf2-dependent mechanisms. *Redox Biol* 2014; 2: 855–864.
6. Ashino T, Yamamoto M and Numazawa S. Nrf2/Keap1 system regulates vascular smooth muscle cell apoptosis for vascular homeostasis: role in neointimal formation after vascular injury. *Sci Rep* 2016; 6: 26291.
7. Al-Jaderi Z and Maghazachi AA. Utilization of dimethyl fumarate and related molecules for treatment of multiple sclerosis, cancer, and other diseases. *Front Immunol* 2016; 7: 278.
8. Scannevin RH, et al. Fumarates promote cytoprotection of central nervous system cells against oxidative stress via the nuclear factor (erythroid-derived 2)-like 2 pathway. *J Pharmacol Exp Ther* 2012; 341: 274–284.

9. Suzuki T and Yamamoto M. Molecular basis of the Keap1-Nrf2 system. *Free Radic Biol Med* 2015; 88(Pt B): 93–100.
10. Nguyen T, Nioi P and Pickett CB. The Nrf2-antioxidant response element signaling pathway and its activation by oxidative stress. *J Biol Chem* 2009; 284: 13291–13295.
11. Villeneuve NF, Lau A and Zhang DD. Regulation of the Nrf2-Keap1 antioxidant response by the ubiquitin proteasome system: an insight into cullin-ring ubiquitin ligases. *Antioxid Redox Signal* 2010; 13: 1699–1712.
12. Ahuja M, et al. Distinct Nrf2 signaling mechanisms of fumaric acid esters and their role in neuroprotection against 1-methyl-4-phenyl-1,2,3,6-tetrahydropyridine-induced experimental Parkinson's-like disease. *J Neurosci* 2016; 36: 6332–6351.
13. Lin SX, et al. The anti-inflammatory effects of dimethyl fumarate in astrocytes involve glutathione and haem oxygenase-1. *ASN Neuro* 2011; 3: e00055. DOI: 10.1042/AN20100033.
14. Yao Y, et al. Dimethyl fumarate and monomethyl fumarate promote post-ischemic recovery in mice. *Transl Stroke Res* 2016; 7: 535–547.
15. Iniaghe LO, et al. Dimethyl fumarate confers neuroprotection by casein kinase 2 phosphorylation of Nrf2 in murine intracerebral hemorrhage. *Neurobiol Dis* 2015; 82: 349–358.
16. Liu Y, et al. Dimethylfumarate alleviates early brain injury and secondary cognitive deficits after experimental subarachnoid hemorrhage via activation of Keap1-Nrf2-ARE system. *J Neurosurg* 2015; 123: 915–923.
17. Kramer T, et al. Dimethyl fumarate treatment after traumatic brain injury prevents depletion of antioxidative brain glutathione and confers neuroprotection. *J Neurochem* 2017; 143: 523–533.
18. Jiang S, et al. Nrf2 weaves an elaborate network of neuroprotection against stroke. *Mol Neurobiol* 2017; 54: 1440–1455.
19. Sawyer DM, et al. Inflammatory mediators in vascular disease: identifying promising targets for intracranial aneurysm research. *Mediators Inflamm* 2015; 2015: 896283.
20. Ali MS, et al. TNF-alpha induces phenotypic modulation in cerebral vascular smooth muscle cells: implications for cerebral aneurysm pathology. *J Cereb Blood Flow Metab* 2013; 33: 1564–1573.
21. Cuadrado A, Kugler S and Lastres-Becker I. Pharmacological targeting of GSK-3 and NRF2 provides neuroprotection in a preclinical model of tauopathy. *Redox Biol* 2018; 14: 522–534.
22. Schulze-Topphoff U, et al. Dimethyl fumarate treatment induces adaptive and innate immune modulation independent of Nrf2. *Proc Natl Acad Sci U S A* 2016; 113: 4777–4782.
23. Nuki Y, et al. Elastase-induced intracranial aneurysms in hypertensive mice. *Hypertension* 2009; 54: 1337–1344.
24. Alam MA, Parks C and Mancarella S. Long-term blood pressure measurement in freely moving mice using telemetry. *J Vis Exp* 2016. DOI: 10.3791/53991.
25. Badhwar A, et al. The proteome of mouse cerebral arteries. *J Cereb Blood Flow Metab* 2014; 34: 1033–1046.
26. Friedman DB. Quantitative proteomics for two-dimensional gels using difference gel electrophoresis. *Methods Mol Biol* 2007; 367: 219–239.
27. Wang Y, et al. Reversed-phase chromatography with multiple fraction concatenation strategy for proteome profiling of human MCF10A cells. *Proteomics* 2011; 11: 2019–2026.
28. Savage RS, et al. Discovering transcriptional modules by Bayesian data integration. *Bioinformatics* 2010; 26: i158–167.
29. Carlson M. *Genome wide annotation for Mouse, in R package version 3.0.0*. 2014: org.Mm.eg.db.
30. Ingenuity systems, Ingenuity pathway analysis, www.ingenuity.com (2012, accessed 10 June 2019).
31. Linker RA, et al. Fumaric acid esters exert neuroprotective effects in neuroinflammation via activation of the Nrf2 antioxidant pathway. *Brain* 2011; 134(Pt 3): 678–692.
32. Chen H, et al. Hydroxycarboxylic acid receptor 2 mediates dimethyl fumarate's protective effect in EAE. *J Clin Invest* 2014; 124: 2188–2192.
33. Girouard MP, et al. RhoA proteolysis regulates the actin cytoskeleton in response to oxidative stress. *PLoS One* 2016; 11: e0168641.
34. Jayaraman T, et al. TNF-alpha-mediated inflammation in cerebral aneurysms: a potential link to growth and rupture. *Vasc Health Risk Manag* 2008; 4: 805–817.
35. Kataoka H. Molecular mechanisms of the formation and progression of intracranial aneurysms. *Neurol Med Chir* 2015; 55: 214–229.
36. Colin-Gonzalez AL, et al. Early modulation of the transcription factor Nrf2 in rodent striatal slices by quinolinic acid, a toxic metabolite of the kynurenine pathway. *Neuroscience* 2014; 260: 130–139.
37. Kanematsu Y, et al. Critical roles of macrophages in the formation of intracranial aneurysm. *Stroke* 2011; 42: 173–178.
38. Wright JL, et al. Cigarette smoke upregulates pulmonary vascular matrix metalloproteinases via TNF-alpha signaling. *Am J Physiol Lung Cell Mol Physiol* 2007; 292: L125–133.
39. Aoki T, et al. Role of TIMP-1 and TIMP-2 in the progression of cerebral aneurysms. *Stroke* 2007; 38: 2337–2345.
40. Ashino T, et al. Redox-sensitive transcription factor Nrf2 regulates vascular smooth muscle cell migration and neointimal hyperplasia. *Arterioscler Thromb Vasc Biol* 2013; 33: 760–768.
41. Gerhardt S, et al. Dimethylfumarate protects against TNF-alpha-induced secretion of inflammatory cytokines in human endothelial cells. *J Inflamm* 2015; 12: 49.
42. Aoki T, et al. Gene expression profile of the intima and media of experimentally induced cerebral aneurysms in rats by laser-microdissection and microarray techniques. *Int J Mol Med* 2008; 22: 595–603.
43. Liu H, et al. Regulation of CCL5 expression in smooth muscle cells following arterial injury. *PLoS One* 2012; 7: e30873.
44. Soehnlein O, et al. Distinct functions of chemokine receptor axes in the atherogenic mobilization and recruitment

of classical monocytes. *EMBO Mol Med* 2013; 5: 471–481.
45. Nowicki KW, et al. Novel high-throughput in vitro model for identifying hemodynamic-induced inflammatory mediators of cerebral aneurysm formation. *Hypertension* 2014; 64: 1306–1313.
46. Jin W, et al. Influence of Nrf2 genotype on pulmonary NF-kappaB activity and inflammatory response after traumatic brain injury. *Ann Clin Lab Sci* 2008; 38: 221–227.
47. Shih AY, Li P and Murphy TH. A small-molecule-inducible Nrf2-mediated antioxidant response provides effective prophylaxis against cerebral ischemia in vivo. *J Neurosci* 2005; 25: 10321–10335.
48. Zhao X, et al. Transcription factor Nrf2 protects the brain from damage produced by intracerebral hemorrhage. *Stroke* 2007; 38: 3280–3286.
49. Lu Q, et al. Signaling through Rho GTPase pathway as viable drug target. *Curr Med Chem* 2009; 16: 1355–1365.
50. Cuadrado A, et al. Transcription factors NRF2 and NF-kappaB are coordinated effectors of the Rho family, GTP-binding protein RAC1 during inflammation. *J Biol Chem* 2014; 289: 15244–15258.
51. Calo LA and Pessina AC. RhoA/Rho-kinase pathway: much more than just a modulation of vascular tone. Evidence from studies in humans. *J Hypertens* 2007; 25: 259–264.
52. Higashi M, et al. Long-term inhibition of Rho-kinase suppresses angiotensin II-induced cardiovascular hypertrophy in rats in vivo: effect on endothelial NAD(P)H oxidase system. *Circ Res* 2003; 93: 767–775.
53. Zhao X, et al. Dimethyl fumarate protects brain from damage produced by intracerebral hemorrhage by mechanism involving Nrf2. *Stroke* 2015; 46: 1923–1928.
54. Cho H, et al. Monomethyl fumarate promotes Nrf2-dependent neuroprotection in retinal ischemia-reperfusion. *J Neuroinflammation* 2015; 12: 239.
55. McGuire VA, et al. Dimethyl fumarate blocks pro-inflammatory cytokine production via inhibition of TLR induced M1 and K63 ubiquitin chain formation. *Sci Rep* 2016; 6: 31159.
56. Ghoreschi K, et al. Fumarates improve psoriasis and multiple sclerosis by inducing type II dendritic cells. *J Exp Med* 2011; 208: 2291–2303.
57. Parodi B, et al. Fumarates modulate microglia activation through a novel HCAR2 signaling pathway and rescue synaptic dysregulation in inflamed CNS. *Acta Neuropathol* 2015; 130: 279–295.
58. Hanson J, et al. Nicotinic acid- and monomethyl fumarate-induced flushing involves GPR109A expressed by keratinocytes and COX-2-dependent prostanoid formation in mice. *J Clin Invest* 2010; 120: 2910–2919.
59. Kornberg MD, et al. Dimethyl fumarate targets GAPDH and aerobic glycolysis to modulate immunity. *Science* 2018; 360: 449–453.